Hedged Deep Tracking

Yuankai Qi[†] Shengping Zhang[†] Lei Qin[♭] Hongxun Yao[†] Qingming Huang[†,♮] Jongwoo Lim[◇] Ming-Hsuan Yang[§]
[†]Harbin Institute of Technology [♭]Institute of Computing Technology, Chinese Academy of Sciences
[♮]University of Chinese Academy of Sciences [◇]Hanyang University [§]University of California at Merced
qykshr@gmail.com s.zhang@hit.edu.cn qinlei@ict.ac.cn h.yao@hit.edu.cn
qmhuang@jdl.ac.cn jlim@hanyang.ac.kr mhyang@ucmerced.edu

Abstract

In recent years, several methods have been developed to utilize hierarchical features learned from a deep convolutional neural network (CNN) for visual tracking. However, as the features from a certain CNN layer characterize an object of interest from only one aspect or one level, the performance of such trackers trained with features from one layer (usually the last second layer) can be further improved. In this paper, we propose a novel CNN based tracking framework, which takes full advantage of features from different CNN layers and uses an adaptive Hedge method to hedge several CNN trackers into a stronger one. Extensive experiments on a benchmark dataset of 100 challenging image sequences demonstrate the effectiveness of the proposed algorithm compared with several state-of-the-art trackers.

1. Introduction

Visual tracking has attracted increasing interest in the past decades due to its importance in numerous applications, such as intelligent video surveillance, vehicle navigation, and human-computer interaction. Despite the significant effort that has been made to develop algorithms [20, 22, 14, 36, 9, 38, 32, 37, 39, 35] and benchmark evaluations [34, 27] for visual tracking, it is still a challenging task owing to complicated interfering factors like heavy illumination changes, shape deformation, partial and full occlusion, large scale variations, in-plane and out-of-plane rotations, and fast motion, to name a few.

Most existing tracking approaches focus on either designing effective decision models [13, 12, 16, 40] or extracting effective features [6, 24, 41, 1]. Recently, inspired by the success of deep convolutional neural networks (CNNs) in object recognition and detection [26, 15, 21, 11], several CNN based trackers [30, 18, 9, 25] have been developed and demonstrated state-of-the-art results on a large object tracking benchmark, compared to methods based on hand-crafted features such as HOG [6], SIFT [24], and color histogram [28, 1].

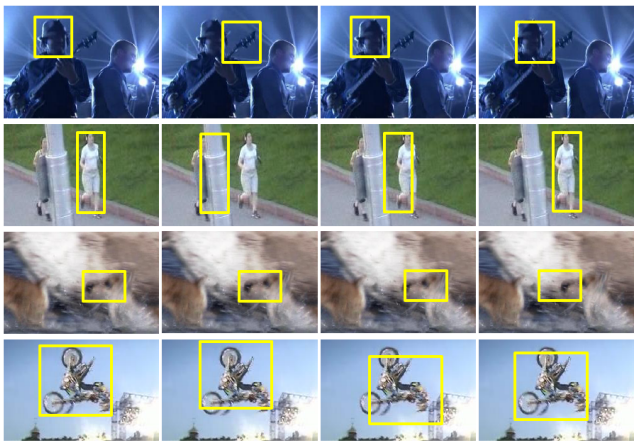

(a) Ground truth (b) VGG layer-10 (c) VGG layer-12 (d) VGG layer-16

Figure 1. Tracking results of using CNN features from different convolutional layers on a representative frame of four sequences with diverse challenges. The best tracking results are obtained using layers 12, 16, 10, and 10 on four sequences, respectively.

Despite achieving state-of-the-art performance, existing CNN trackers still have some limitations. Most of these methods only use the features from the last layers (*e.g.* fully-connected layers) of CNNs to represent target objects. Although features from deeper layers capture rich category-level semantic information, which is useful for object classification, they are not the optimal representation for visual tracking since spatial details captured by earlier layers are also important for accurately localizing the targets as shown in the last two cases in Figure 1. On the other hand, as the features in the earlier layers are more generic rather than discriminative as ones in the later layers, methods based on features from earlier layers are likely to fail in challenging scenarios, such as the first two cases shown in Figure 1. To achieve better tracking performance, it is thus imperative to combine features from different layers to best represent and separate foreground objects from the background clutters.

In this paper, we propose a novel CNN based tracking algorithm, which first builds a weak tracker from a convolutional layer by applying a correlation filter on the layer output, and then hedges all weak trackers into a stronger one by using an online decision-theoretical Hedge algorithm. Specifically, we treat each weak tracker as an expert and compute weights to all experts as their decision confidences. The tracking result in current frame is the weighted decision of all experts, which combines advantages of all considered CNN layers. Since the tracked target moves a small offset between consecutive frames and undergoes appearance variance gradually, the experts that perform well in previous frames may still perform well in current frame with high probability. By factoring in the historical performance of experts to make decisions, we propose an improved Hedge algorithm to update the weights of experts, which is more suitable for real-world tracking tasks.

The contributions of this paper are summarized below:

- We propose a novel tracking algorithm that combines weak CNN trackers from numerous convolutional layers into a stronger tracker.
- We develop an improved Hedge algorithm for visual tracking by considering historical performance of weak trackers.
- We carry out extensive experiments on a large-scale benchmark dataset [34] with 100 challenging sequences to demonstrate the effectiveness of the proposed algorithm with comparisons to the state-of-the-art trackers.

2. Related Work

We give a brief review of tracking methods closely related to this work. Comprehensive reviews on visual tracking approaches can be found in [23, 27].

Correlation filters based trackers. Correlation filters are introduced into visual tracking for its high computational efficiency [4, 16, 17]. These methods approximate the dense sampling scheme by generating a circulant matrix, of which each row denotes a vectorized sample. As such, its regression model can be computed in the Fourier domain, which brings hundreds of times speed improvement in both training and testing stages. Bolme *et al*. [4] develop the Minimum Output Sum of Squared Error (MOSSE) method to learn the filters, and use intensity features for object representation. In [16], Henriques *et al*. propose a tracking method based on correlation filters by introducing kernel methods and employing ridge regression. Subsequently a method that extends the input features from single channel to multiple channels (*e.g*., HOG) is presented [17]. Danelljan *et al*. [7] propose an algorithm that searches over scale space for correlation filters to handle large variation in object size. However, all above mentioned works use only one correlation filter, which limits the power of correlation filtered trackers. In this work, we exploit the high computational efficiency of correlation filters to construct an ensemble tracker where each is based on CNN features extracted from one convolutional layer.

CNN based trackers. Hierarchical features learned from convolutional neural networks have been shown to be effective for numerous vision tasks, *e.g*., classification and recognition [21, 26, 15] in recent years. Numerous methods have since been proposed to exploit CNN features [9, 30, 18] for visual tracking. In [9], Fan *et al*. utilize a pre-trained deep network for human tracking. Wang and Yeung [30] design an autoencoder network to learn representative features for generic objects. Hong *et al*. [18] construct a discriminative model with features from the first fully-connected layer of R-CNN [11] and a generative model with saliency map for visual tracking. While this method is effective for visual tracking, the computational complexity is high. We note the above mentioned methods do not exploit the features from different layers adequately. As shown in Figure 1, features from different layers are effective for different scenarios. Based on these observations, we use an ensemble of multiple CNN trackers where each one is trained with CNN features from one layer. We regard each one as a weak expert and hedge them adaptively for visual tracking.

Ensemble trackers. Ensemble approaches have been developed to exploit multiple experts for visual tracking. Numerous ensemble tracking methods [2, 31, 12, 3] have been developed based on hand-crafted features. In this paper, we combine weak trackers based on features from different CNN layers. Existing ensemble methods [2, 12, 3] under the boosting framework [10] incrementally build an ensemble, which trains each new weak tracker to emphasize the training samples that previous trackers mis-classified. In [31], Wang and Yeung use a conditional particle filter to infer the target position and the reliability of each member tracker. Different from these works, we consider visual tracking as a decision-theoretic online learning task [5] based on multiple expert trackers. That is, in every round each expert makes a decision and the final decision is determined by weighted decision of all experts.

3. Algorithmic Overview

As shown in Figure 2, the proposed approach consists of three steps: extracting CNN features, constructing weak trackers, and hedging weak trackers. The pre-trained VGG-Net [26] is used to extract feature maps of convolutional layers from the interested image region, which represent the tracked target at different resolutions and semantic levels. Each feature map is then convoluted by correlation filters to generate response maps, from which a weak tracker is constructed with moderate performance. All weak trackers are

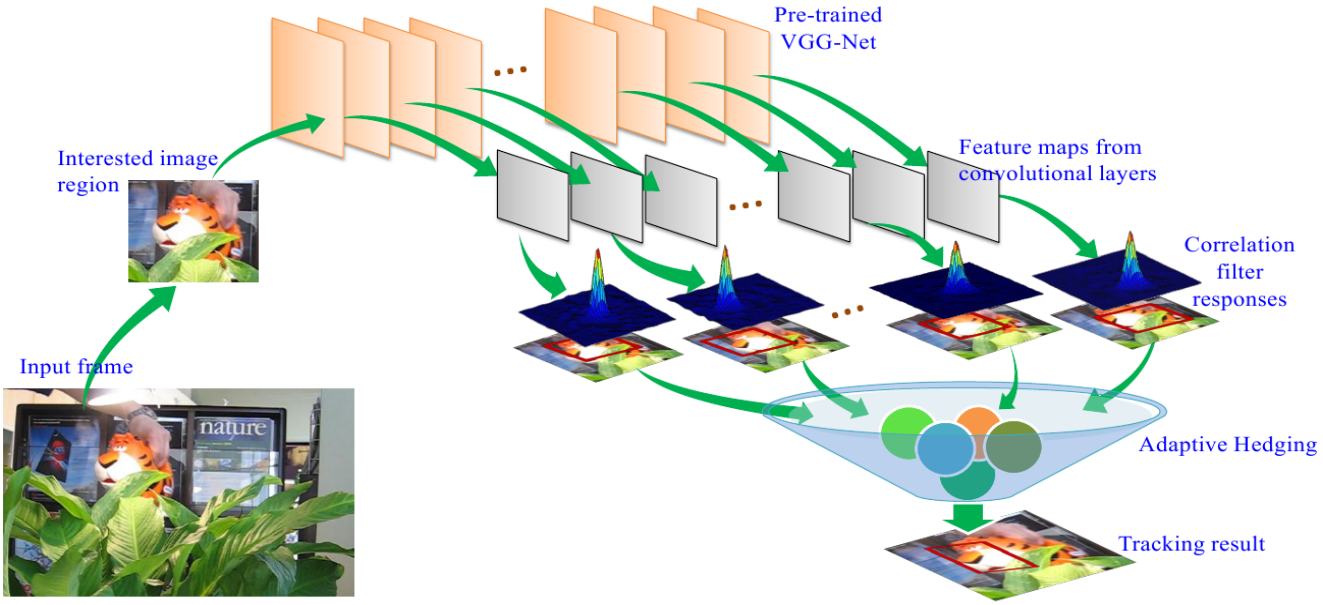

Figure 2. Main steps of the proposed algorithm. The proposed algorithm consists of three components: 1) extracting CNN features from different convolutional layers using the pre-trained VGG-Net (Section 4.1); 2) constructing weak trackers using correlation filters where each one is trained with CNN features from one layer (Section 4.2); 3) hedging weak trackers into a stronger one using an improved Hedge algorithm (Section 4.3).

finally hedged into a stronger tracker by the proposed adaptive Hedge algorithm for visual tracking, which exploits the strength of all CNN layers for robust performance.

4. Proposed Algorithm

In this section, we first present the technical details of the proposed algorithm and then describe the online update scheme.

4.1. Deep CNN features

Numerous CNN models, such as AlexNet [21], R-CNN [11], CaffeNet [19], and VGG-Net [26], have been developed for large-scale image classification and object recognition tasks. The proposed method is based on the VGG-Net, as it has a much deeper architecture (up to 19 weight layers) and hence can provide features from more levels compared to most CNNs which usually have 5 or 7 layers. The VGG-Net is trained using 1.3 million images of the ImageNet dataset and achieves the state-of-the-art results on classification challenges [26].

Different from classification tasks which only require the extracted features to capture more category-level semantic information, visual tracking also requires the extracted features to have precise localization ability since a small drift from the tracked target to its surrounding background causes gradual degradation in tracking performance and eventual failure. The deep VGG-Net facilitates features extracted from different layers to describe target objects with greater details. In other words, tracking methods using CNN features from any layer alone is less effective (see Figure 1 for example of tracking failures).

4.2. Weak CNN trackers

In this work, a module based on correlation filters on CNN features extracted from one layer is considered as a weak tracker. Correlation filters based trackers [4, 7, 17, 16] exploit the circulant structure of training and testing samples to greatly accelerate the training and testing processes with negligible precision loss. Let $X^k \in \mathbb{R}^{P\times Q\times D}$ denotes the feature map extracted from the k-th convolutional layer; $Y \in \mathbb{R}^{P\times Q}$ denotes a gaussian shape label matrix, which is subject to a 2D Gaussian distribution with zero mean and standard deviation proportional to the target size; and $\mathcal{X}^k = \mathcal{F}(X^k)$, $\mathcal{Y} = \mathcal{F}(Y)$, where $\mathcal{F}(\cdot)$ denotes discrete Fourier transformation (DFT). The k-th filter can be modeled in the Fourier domain by

$$\mathcal{W}^k = \arg\min_{\mathcal{W}} \|\mathcal{Y} - \mathcal{X}^k \bullet \mathcal{W}\|_F^2 + \lambda\|\mathcal{W}\|_F^2, \qquad (1)$$

where

$$\mathcal{X}^k \bullet \mathcal{W} = \sum_{d=1}^{D} \mathcal{X}^k_{*,*,d} \odot \mathcal{W}_{*,*,d}, \qquad (2)$$

and the symbol $\odot$ denotes element-wise product.

The optimization problem in (1) has a simple closed form solution, which can be efficiently computed in the Fourier domain by

$$\mathcal{W}^k_{*,*,d} = \frac{\mathcal{Y}}{\mathcal{X}^k \bullet \mathcal{X}^k + \lambda} \odot \mathcal{X}^k_{*,*,d}. \qquad (3)$$

Given the testing data T^k from the output of the k-th layer, we first transform it to the Fourier domain $\mathcal{T}^k = \mathcal{F}(T^k)$, and then the responses can be computed by

$$S^k = \mathcal{F}^{-1}(\mathcal{T}^k \bullet \mathcal{W}^k), \tag{4}$$

where $\mathcal{F}^{-1}$ denotes the inverse of DFT.

The k-th weak tracker outputs the target position with the largest response

$$(x^k, y^k) = \arg\max_{x',y'} S^k(x', y'). \tag{5}$$

4.3. Hedging CNN trackers

The standard parameter-free Hedge algorithm [5] is proposed to tackle the decision-theoretic online learning problem in a multi-expert multi-round setting. Given the initial confidence weights on all experts, in the current round, a final decision is made based on weighted decisions of all experts. The weights of experts are then updated to reflect each expert's decision loss. In the visual tracking scenario, it is natural to treat each CNN tracker as an expert and then predict the target position in the t-th frame by

$$(x_t^*, y_t^*) = \sum\nolimits_{k=1}^{K} w_t^k \cdot (x_t^k, y_t^k), \tag{6}$$

where w_t^k is the weight of expert k and $\sum_{k=1}^{K} w_t^k = 1$. Once the ultimate target position is predicted, each expert will incur a loss.

Let

$$\ell_t^k = \max(S_t^k) - S_t^k(x_t^*, y_t^*) \tag{7}$$

be the loss suffered by expert k at frame t, where $\max(\cdot)$ operates on a matrix and returns the largest element of the matrix and $S(x, y)$ denotes the element at position (x, y) of matrix S. The standard parameter-free Hedge algorithm generates a new weight distribution on all experts by introducing a *regret* measure defined by

$$r_t^k = \bar{\ell}_t^k - \ell_t^k, \tag{8}$$

where the weighted average loss among all experts is computed as $\bar{\ell}_t^k = \sum_{k=1}^{K} w_t^k \ell_t^k$.

By optimizing the cumulative regret

$$R_t^k = \sum\nolimits_{\tau=1}^{t} r_\tau^k, \tag{9}$$

to any expert k, for any round of t, the new weights $w_{t+1}^1, \cdots, w_{t+1}^K$ are generated.

Although the standard parameter-free Hedge algorithm performs well in the simulated one-dimension tracking experiment, where the target stays stationary or moves in a constant velocity [5], it is less effective for the real-world tracking tasks since it does not consider two crucial factors: (i) The target appearance usually changes at irregular pace (sometimes gradually and sometimes rapidly). This means the proportion of the historic regret R_{t-1}^k should vary with time t to better reflect the current state for visual tracking. (ii) Since each expert captures a different aspect of the target, it is not effective to fix the ratio of the cumulative regret over all experts. To address these issues, we propose an adaptive Hedge algorithm, which considers the difference of historic regrets over time t and expert k simultaneously.

As the object appearance usually does not change significantly at least in a short time period, we model the loss of each expert ℓ^k during time period Δt via a Gaussian distribution with mean μ_t^k and standard variance σ_t^k

$$\mu_t^k = \frac{1}{\Delta t} \sum_{\tau=t-\Delta t+1}^{t} \ell_\tau^k, \tag{10}$$

$$\sigma_t^k = \sqrt{\frac{1}{\Delta t - 1} \sum_{\tau=t-\Delta t+1}^{t} (\ell_\tau^k - \mu_t^k)^2}. \tag{11}$$

We then measure the stability of expert k at time t using

$$s_t^k = \frac{|\ell_t^k - \mu_t^k|}{\sigma_t^k}. \tag{12}$$

A smaller s_t^k indicates that this expert tends to be more stable than the one with a larger s_t^k, and therefore we prefer a larger proportion on its current regret. In contrast, a larger s_t^k means this expert varies greatly, and therefore we compute its cumulative regret mainly depending on its historic information. Based on this principle, we obtain the following adaptive cumulative regret

$$R_t^k = (1 - \alpha_t^k) R_{t-1}^k + \alpha_t^k r_t^k, \tag{13}$$

$$\alpha_t^k = \min\left(g, \exp\left(-\gamma s_t^k\right)\right), \tag{14}$$

where γ is a scale factor and g defines a maximum ratio on current regret to avoid that no historic information is considered. We validate the effectiveness of the proposed adaptive Hedge compared to the original one in Section 5.4.

Since our adaptive Hedge algorithm adheres to the framework of the standard one, the solution to minimize the cumulative regret (13) has the same form,

$$w_{t+1}^k \propto \frac{[R_t^k]_+}{c_t} \exp \frac{([R_t^k]_+)^2}{2c_t}, \tag{15}$$

where $[R_t^k]_+$ denotes $\max\{0, R_t^k\}$, and c_t servers as a scale parameter like in [5], which is determined by solving $\frac{1}{K}\sum_{k=1}^{K} \exp(\frac{([R_t^k]_+)^2}{2c_t}) = e$.

4.4. Model update

Since the feature maps of VGG-Net have up to 512 channels, retraining of ridge regression models with newly collected samples is impractical, especially when the amount

Algorithm 1: Hedged deep tracking

Input: initial weights $w_1^1, \cdots, w_1^K$; target position (x_1, y_1) in the 1st frame; VGG-Net19; $R_1^k = 0, \ell_1^k = 0$;
Crop interested image region;
Initiate K weak experts using (3);
for $t = 2, 3, \cdots$ **do**
  Exploit the VGG-Net19 to obtain K representations;
  Compute correlation filter responses using (4);
  Find target position predicted by each expert using (5);
  if $t \neq 2$ **then**
    Compute ultimate location using (6);
  else
    Set ultimate location with ground truth;
  end
  Compute experts' losses using (7);
  Update stability models using (10) and (11);
  Measure each expert's stability using (12);
  Compute adaptive proportion of historic regret for each expert using (14);
  Update cumulative regret of each expert using (13);
  Update weights for each expert using (15) and normalize them to have a sum of 1;
end

of the training data becomes extremely large over time. In practice, we adopt an incremental update manner like that in [7], which only uses new samples $\bar{\mathcal{X}}^k$ in the current frame to partially update the existed models,

$$\mathcal{Z}_{*,*,d}^k = \frac{\mathcal{Y}}{\bar{\mathcal{X}}^k \bullet \bar{\mathcal{X}}^k + \lambda} \odot \bar{\mathcal{X}}_{*,*,d}^k, \quad (16)$$

$$\mathcal{W}_t^k = (1-\eta)\mathcal{W}_{t-1}^k + \eta \mathcal{Z}_t^k. \quad (17)$$

Algorithm 1 summarizes the main steps of the proposed approach for visual tracking.

5. Experimental Results

In this section, we present extensive experimental evaluations on the proposed hedged deep tracker (HDT). We first discuss the implementation details and the evaluation protocol. We present two sets of experimental evaluations: one compared with several state-of-the-art trackers and the other one compared with several baseline trackers including individual weak trackers and the hedged strong tracker using the standard parameter-free Hedge method [5].

5.1. Implementation details

For feature extraction, we crop an image patch with 2.2 times the size of the target bounding box and then resize it to 224×224 pixels for the VGG-Net with 19 layers (16 convolutional layers and 3 fully-connected layers). After the forward propagation, we use the outputs from six convolutional layers (10th∼12th, 14th∼16th) as six types of

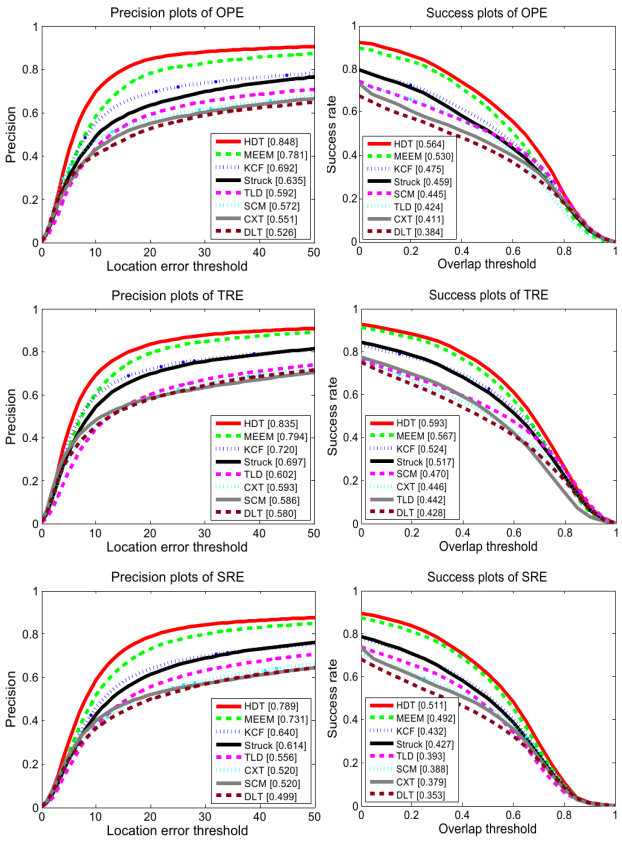

Figure 3. Evaluation results on 100 sequences.

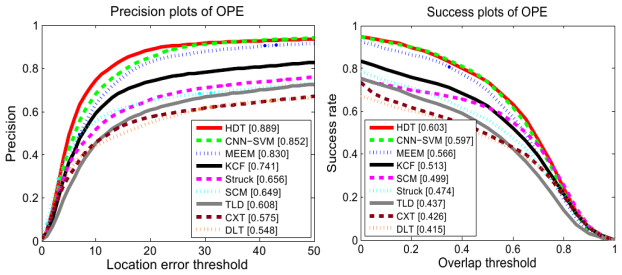

Figure 4. Evaluation results on 50 sequences.

features and all feature maps are resized to a same size. This setting simultaneously takes the feature's diversity and the computational cost into consideration. Since VGG-Net adopts very small convolutional filters (3×3 pixel size), the feature maps from shallower layers (*i.e.*, less than 10) have limited representation strength (see Section 5.4). We implement our algorithm in MATLAB, and utilize the MatConvNet toolbox [29] in this work. Our implementation runs at 10 frames per second on a computer with an Intel I7-4790K 4.00 GHz CPU, 16GB RAM, and a GeForce GTX780Ti GPU card which is only used to compute the CNN features. We will make MATLAB code available to the public.

All the following experiments are carried out with the

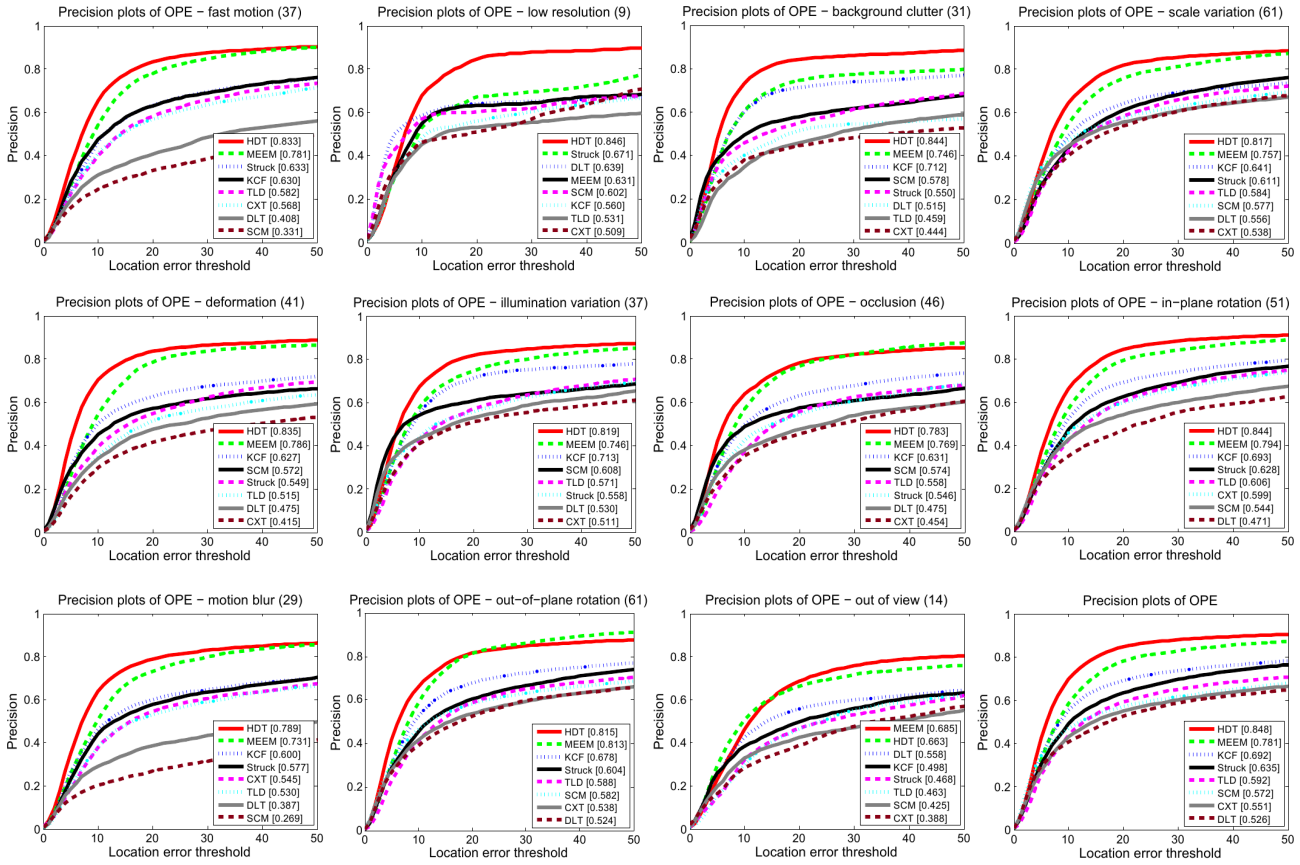

Figure 5. Attribute-based evaluation on 100 sequences. We also put the overall performance here (the last one) for comparison convenience facing a single challenge and their combination.

fixed parameters: the tradeoff parameter in (1) is set to $\lambda = 10^{-4}$; the time window in (10) is set to $\Delta t = 5$; the truncate threshold in (14) is set to $g = 0.97$; the learning rate in (17) is set to $\eta = 0.01$; and the initial weights of the six weak experts are empirically set to (1, 0.2, 0.2, 0.02, 0.03, 0.01).

5.2. Evaluation protocol

To fully assess our method, we use one-pass evaluation (OPE), temporal robustness evaluation (TRE), and spatial robustness evaluation (SRE) metrics on a large object tracking benchmark dataset [34] which contains 100 image sequences. These sequences involve 11 tracking challenging factors, such as illumination changes, camera shake, scale variation, pose variation, partial or full occlusion, and rotation, to name a few. Experimental results are reported using overlap success plots and center location error plots, which rank trackers in terms of area under the curve and distance precision at threshold 20 pixels, respectively. For completeness, we also report the results on the benchmark [33], which is a subset of [34]. More results and videos are presented in the supplementary material.

5.3. Comparison with state-of-the-art trackers

We compare our algorithm with 8 recent state-of-the-art trackers: DLT [30], CNN-SVM [18], KCF [17], MEEM [36], Struck [14], CXT [8], TLD [20], and SCM [41]. The first two trackers are based on deep learning; KCF is one of the best correlation filters based trackers; and the remaining trackers rank top 5 in benchmark [34].

Quantitative evaluation. Figure 3 shows the OPE, TRE, and SRE evaluation results on 100 image sequences. We note that the results from CNN-SVM are not included as the source code is not available for fair comparisons. On the other hand, we also provide a comparison on 50 sequences in Figure 4 where only OPE results of CNN-SVM are reported in [18]. Figure 3 and Figure 4 show that our HDT performs favorably against the state-of-the-art methods on all the three evaluation metrics. We note that HDT performs better in terms of precision metric (than overlap), which indicates that HDT can track target objects well but give a less accurate bounding box since, for computational efficiency, HDT does not search over scales to determine the best one.

Figure 6. Bounding box comparison on several challenging image sequences (from left to right and top to down are *bolt2, coke, diving, dragonBaby, football, human2, human9, ironman, shaking, and trellis*, respectively).

Learned parameters by standard Hedge

	Left	Top	Alpha	R	Weight
VGG-16	427.11	144.31	--	0.0193	0.04
VGG-15	427.11	144.31	--	-0.2243	0.00
VGG-14	435.11	160.31	--	-0.1248	0.00
VGG-12	435.11	160.31	--	0.0770	0.81
VGG-11	439.11	160.31	--	0.0371	0.09
VGG-10	439.11	160.31	--	0.0286	0.06
Final	435.39	159.67	--	--	--

Learned parameters by our adaptive Hedge

	Left	Top	Alpha	R	Weight
VGG-16	426.64	144.02	0.1190	0.0063	1.00
VGG-15	426.64	144.02	0.1190	-0.0343	0.00
VGG-14	434.64	160.02	0.1985	-0.0222	0.00
VGG-12	434.64	160.02	0.1190	-0.0374	0.00
VGG-11	438.64	160.02	0.1190	-0.0774	0.00
VGG-10	439.64	160.02	0.1190	-0.0749	0.00
Final	426.64	144.02	--	--	--

Figure 7. Tracking results on the 12-th frame of the *skiing* sequence. We illustrating how the weights are assigned to the CNN trackers by the proposed adaptive and the standard parameter-free Hedge methods.

Attribute-based evaluation. To thoroughly evaluate the robustness of the proposed HDT in various scenes, we summarize the performance based on 11 different challenging factors on 100 image sequences. As illustrated in Figure 5, our algorithm performs well against the other methods in almost all tracking attributes. In particular, HDT outperforms other methods by a huge margin in handling low resolution, which can be attributed to CNN features with rich spatial details from earlier layers and features with semantics from later layers. In contrast, DLT only takes advantage of deeper features, and hence its performance is suffered. We also observed that HDT does not perform well in handling out-of-view challenge, which can be explained as that HDT does not search for the target in a whole frame to reduce computational load, and therefore HDT may lose the target which may reappears somewhere else.

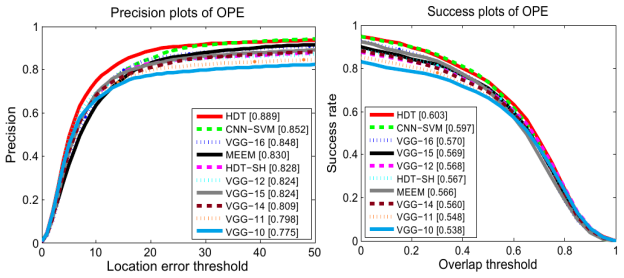

Figure 8. Comparison among the proposed algorithm and several baselines: all its constituent CNN trackers and the one combined by standard parameter-free Hedge. For completeness, we also include two state-of-the-art methods, CNN-SVM and MEEM, in the plots.

Qualitative evaluation. We present some tracking results from the evaluated methods in Figure 6, where challenging frames among 100 image sequences are selected. For presentation clarity, the results by the top six performing methods are shown. Overall, our tracker can localize the targets more precisely. Other methods, however, almost can not handle these complicated scenarios. The MEEM tracker performs well in presence of illumination variations, occlusion, and in-plane-rotation (*shaking, coke,* and *trellis*), which can be explained as that MEEM simultaneously maintains several target snapshots at different times. However, it tends to fail when similar objects appear, such as *bolt2* and *football*, since the features are not discriminative enough. When the background is quite cluttered, like sequences *diving* and *ironman*, most of the compared methods are apt to lose the target. Although DLT adopts a deep autoencoder network, it generally falls in failure on these challenging sequences. This mainly attributes to that its deep network has no shared weights and it is trained with small amounts of data. Since our HDT hedges several weak CNN trackers that perform well in different environments, it can overcome these challenges much better than other trackers. In addition, we note that in the *diving, human9,* and *trellis* sequences, even though HDT tracks targets accurately, some of its bounding boxes are not tight since it does not search for the best scale as previously discussed.

5.4. Comparison with baseline trackers

To evaluate the effectiveness of the proposed adaptive Hedge method, we compare the HDT with its constituent CNN trackers denoted by VGG-10, VGG-11, VGG-12, VGG-14, VGG-15, and VGG-16, as well as the hedged CNN tracker using the standard parameter-free Hedge [5], denoted by HDT-SH, on the benchmark [33].

Figure 8 shows the tracking results. When the CNN features from each convolutional layer are used solely for tracking, the performance generally increases as the layer depth is increased. But even the best individual CNN tracker VGG-16 still does not perform as well as CNN-SVM. This is because CNN-SVM takes advantages of both a R-CNN feature based discriminative model (feature of fc_6 is used) and a back-project saliency map based generative model. Note that the performance of VGG-10 is far behind that of MEEM which is based on hand-crafted features. This explains why we train weak trackers only using convolutional features from layers no shallower than 10th. When combining these six individual CNN trackers using the standard Hedge, the tracking performance is worse than the best performed individual tracker. In contrast, the proposed HDT achieves the best results, which demonstrates the effectiveness of the adaptive Hedge method.

To further explore the difference between the proposed adaptive and the standard parameter-free Hedge methods, we present a comparison of them on a typical frame at running time in Figure 7. Figure 7 shows that the proposed adaptive Hedge method allocates more desirable weights to weak CNN trackers than the standard one. The reason mainly lies in the computation of the accumulative regret R. The standard Hedge scheme uses a fixed proportion of historical information R_{t-1} for all weak trackers at any time t. In contrast, we adaptively compute the proportion of historical information R_{t-1}, *i.e.* we introduce a dynamic parameter α in (13) and model the α with a Gaussian distribution in a time window Δt. As demonstrated in Figure 8, the hedged tracker using the adaptive scheme performs better.

6. Conclusion

In this paper, we propose a novel CNN based tracking framework which uses an adaptive online decision learning algorithm to hedge weak trackers, obtained using correlation filters on CNN feature maps, into a stronger one to achieve better results. To the best of our knowledge, the proposed algorithm is the first to adaptively hedge features from different CNN layers in an online manner for visual tracking. Extensive experimental evaluations on a large-scale benchmark dataset demonstrate the effectiveness of the proposed hedged deep tracking algorithm.

7. Acknowledgments

This work was supported in part by National Basic Research Program of China (973 Program) 2015CB351802 and 2012CB316400, in part by National Natural Science Foundation of China 61332016, 61025011, 61133003, 61472103, 61390510, 61572465, and 61300111. J. Lim is supported partly by R&D programs by NRF (2014R1A1A2058501) and MSIP/NIPA (H8601-15-1005). M.-H. Yang is supported in part by the National Science Foundation CAREER Grant 1149783 and IIS Grant 1152576, and a gift from Adobe.

References

[1] A. Adam, E. Rivlin, and I. Shimshoni. Robust fragments-based tracking using the integral histogram. In *CVPR*, 2006. 1

[2] S. Avidan. Ensemble tracking. *TPAMI*, 29(2):261–271, 2007. 2

[3] Q. Bai, Z. Wu, S. Sclaroff, M. Betke, and C. Monnier. Randomized ensemble tracking. In *ICCV*, 2013. 2

[4] D. S. Bolme, J. R. Beveridge, B. A. Draper, and Y. M. Lui. Visual object tracking using adaptive correlation filters. In *CVPR*, 2010. 2, 3

[5] K. Chaudhuri, Y. Freund, and D. Hsu. A parameter-free hedging algorithm. In *NIPS*, 2009. 2, 4, 5, 8

[6] N. Dalal and B. Triggs. Histograms of oriented gradients for human detection. In *CVPR*, 2005. 1

[7] M. Danelljan, G. Häger, F. S. Khan, and M. Felsberg. Accurate scale estimation for robust visual tracking. In *BMVC*, 2014. 2, 3, 5

[8] T. B. Dinh, N. Vo, and G. G. Medioni. Context tracker: Exploring supporters and distracters in unconstrained environments. In *CVPR*, 2011. 6

[9] J. Fan, W. Xu, Y. Wu, and Y. Gong. Human tracking using convolutional neural networks. *TNN*, 21(10):1610–1623, 2010. 1, 2

[10] Y. Freund and R. E. Schapire. A desicion-theoretic generalization of on-line learning and an application to boosting. In *Computational learning theory*, 1995. 2

[11] R. B. Girshick, J. Donahue, T. Darrell, and J. Malik. Rich feature hierarchies for accurate object detection and semantic segmentation. In *CVPR*, 2014. 1, 2, 3

[12] H. Grabner, M. Grabner, and H. Bischof. Real-time tracking via on-line boosting. In *BMVC*, 2006. 1, 2

[13] H. Grabner, C. Leistner, and H. Bischof. Semi-supervised on-line boosting for robust tracking. In *ECCV*, 2008. 1

[14] S. Hare, A. Saffari, and P. H. S. Torr. Struck: Structured output tracking with kernels. In *ICCV*, 2011. 1, 6

[15] K. He, X. Zhang, S. Ren, and J. Sun. Spatial pyramid pooling in deep convolutional networks for visual recognition. In *ECCV*, 2014. 1, 2

[16] J. F. Henriques, R. Caseiro, P. Martins, and J. Batista. Exploiting the circulant structure of tracking-by-detection with kernels. In *ECCV*, 2012. 1, 2, 3

[17] J. F. Henriques, R. Caseiro, P. Martins, and J. Batista. High-speed tracking with kernelized correlation filters. *TPAMI*, 37(3):583–596, 2015. 2, 3, 6

[18] S. Hong, T. You, S. Kwak, and B. Han. Online tracking by learning discriminative saliency map with convolutional neural network. In *ICML*, 2015. 1, 2, 6

[19] Y. Jia, E. Shelhamer, J. Donahue, S. Karayev, J. Long, R. B. Girshick, S. Guadarrama, and T. Darrell. Caffe: Convolutional architecture for fast feature embedding. In *ACM Multimedia*, 2014. 3

[20] Z. Kalal, J. Matas, and K. Mikolajczyk. P-N learning: Bootstrapping binary classifiers by structural constraints. In *CVPR*, 2010. 1, 6

[21] A. Krizhevsky, I. Sutskever, and G. E. Hinton. Imagenet classification with deep convolutional neural networks. In *NIPS*, 2012. 1, 2, 3

[22] G. Li, L. Qin, Q. Huang, J. Pang, and S. Jiang. Treat samples differently: Object tracking with semi-supervised online covboost. In *ICCV*, 2011. 1

[23] X. Li, W. Hu, C. Shen, Z. Zhang, A. R. Dick, and A. van den Hengel. A survey of appearance models in visual object tracking. *ACM TIST*, 4(4):58, 2013. 2

[24] D. G. Lowe. Object recognition from local scale-invariant features. In *ICCV*, 1999. 1

[25] C. Ma, J.-B. Huang, X. Yang, and M.-H. Yang. Hierarchical convolutional features for visual tracking. In *ICCV*, 2015. 1

[26] K. Simonyan and A. Zisserman. Very deep convolutional networks for large-scale image recognition. *CoRR*, abs/1409.1556, 2014. 1, 2, 3

[27] A. W. M. Smeulders, D. M. Chu, R. Cucchiara, S. Calderara, A. Dehghan, and M. Shah. Visual tracking: An experimental survey. *TPAMI*, 36(7):1442–1468, 2014. 1, 2

[28] G. Tian, R. Hu, Z. Wang, and Y. Fu. Improved object tracking algorithm based on new HSV color probability model. In *ISNN*, 2009. 1

[29] A. Vedaldi and K. Lenc. Matconvnet: Convolutional neural networks for MATLAB. In *ACM Multimedia*, 2015. 5

[30] N. Wang and D.-Y. Yeung. Learning a deep compact image representation for visual tracking. In *NIPS*, 2013. 1, 2, 6

[31] N. Wang and D.-Y. Yeung. Ensemble-based tracking: Aggregating crowdsourced structured time Series data. In *ICML*, 2014. 2

[32] L. Wen, D. Du, Z. Lei, S. Li, and M.-H. Yang. Jots: Joint online tracking and segmentation. In *CVPR*, 2015. 1

[33] Y. Wu, J. Lim, and M.-H. Yang. Online object tracking: A benchmark. In *CVPR*, 2013. 6, 8

[34] Y. Wu, J. Lim, and M.-H. Yang. Object tracking benchmark. *TPAMI*, 37:1834–1848, 2015. 1, 2, 6

[35] B. Zhang, A. Perina, Z. Li, V. Murino, J. Liu, and R. Ji. Bounding multiple gaussians uncertaninty with application to object tracking. *IJCV*, pages 1–16, 2016. 1

[36] J. Zhang, S. Ma, and S. Sclaroff. MEEM: robust tracking via multiple experts using entropy minimization. In *ECCV*, 2014. 1, 6

[37] S. Zhang, S. Kasiviswanathan, P. C. Yuen, and M. Harandi. Online dictionary learning on symmetric positive definite manifolds with vision applications. In *AAAI*, 2015. 1

[38] S. Zhang, H. Yao, X. Sun, and X. Lu. Sparse coding based visual tracking: Review and experimental comparison. *Pattern Recognition*, 46:1772–1788, 2013. 1

[39] S. Zhang, H. Zhou, F. Jiang, and X. Li. Robust visual tracking using structurally random projection and weighted least squares. *IEEE Trans. Circuits Syst. Video Techn.*, 25:1749–1760, 2015. 1

[40] T. Zhang, B. Ghanem, S. Liu, and N. Ahuja. Robust visual tracking via multi-task sparse learning. In *CVPR*, 2012. 1

[41] W. Zhong, H. Lu, and M.-H. Yang. Robust object tracking via sparsity-based collaborative model. In *CVPR*, 2012. 1, 6